Available online at www.sciencedirect.com

ScienceDirect

Mendeleev Commun., 2019, **29**, 395–397

Mendeleev Communications

Skeleton pseudomorphs of nanostructured silver for the surface-enhanced Raman spectroscopy

Anna A. Semenova,[a] Sergey V. Savilov,[b] Alexander E. Baranchikov,[c] Vladimir K. Ivanov[a,c] and Eugene A. Goodilin*[a,b,c]

[a] *Department of Materials Science, M. V. Lomonosov Moscow State University, 119991 Moscow, Russian Federation. Fax: +7 495 939 0998; e-mail: goodilin@yandex.ru*

[b] *Department of Chemistry, M. V. Lomonosov Moscow State University, 119991 Moscow, Russian Federation*

[c] *N. S. Kurnakov Institute of General and Inorganic Chemistry, Russian Academy Sciences, 119991 Moscow, Russian Federation*

DOI: 10.1016/j.mencom.2019.07.012

Pseudomorphs (mesocages) of metallic silver were prepared *via* either a shape-preserving reduction of polyhedral Ag_2O precursors with H_2O_2 in aqueous ammonia or an ultrasonic spray pyrolysis of aqueous diamminesilver(I) hydroxide. Both the materials were revealed as suitable for the direct analysis at 0.1–1 μM concentrations of oil pollutants and pharmaceutical substances using surface-enhanced Raman spectroscopy due to their unique morphology providing either a larger surface area for sorption of analytes or additional 'hot spots' resulting in the enhancement factors of 10^6–10^8.

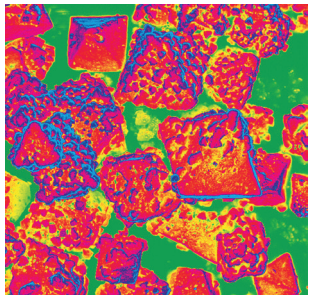

Silver nanoparticles are highly demanded in practical applications as catalysts, conducting and biologically active materials,[1–5] building units for nanoscale devices, in flexible electronics,[6,7] and, especially, in modern devices utilizing highly sensitive assays by the surface-enhanced Raman spectroscopy (SERS).[8–13] Seeding, aggregation-based growth, kinetically controlled overgrowth, template-directed methods, selective etching, and ageing have been developed for the preparation of Ag nanoparticles (NPs) possessing controlled morphologies.[1–4,9] These nanostructures are efficient probes for SERS of biologically active molecules, oncologic markers, living cells and their compartments in the frame of development of new medical screening procedures and personal medicine.[1,9,14–19] Pseudomorphs are defined as the result of shape-preserving processes of phase transformations. They are further promising as SERS-active materials due to the expected broader light absorption spectral range as compared to narrow plasmonic bands of separated Ag NPs and their enhanced surface area being available for target sensing of adsorbed substances.[13,20]

Here, we report on both the optimization of controlled synthesis of silver pseudomorphic particles[†] (Figure 1)[13,20,‡] to yield a large fraction of porous octahedra with morphologically predetermined hot spots and the ensemble of randomized polyhedral Ag NPs (Figure 2) produced by aerosol decomposition and self-etching.[§]

An overall morphology of the polyhedra prepared according to the PVP protocol demonstrates features of nucleation and

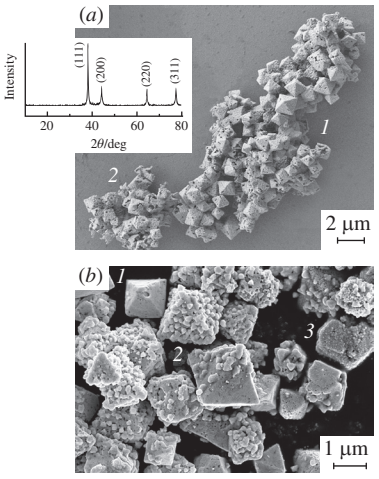

Figure 1 SEM images of metallic silver nanostructured particles obtained by pseudomorphic reduction of octahedral Ag_2O precursor with hydrogen peroxide: (*a*) the general view of precipitate (the inset shows an XRD pattern of cubic silver) and (*b*) the magnified view of porous polyhedral particles showing (*1*) the smooth morphology, (*2*) octahedra overgrown with Ag NPs, and (*3*) intergrown pseudomorphic silver.

[†] At the first step, octahedral Ag_2O was formed upon the treatment of aqueous solution of $AgNO_3$ (50 ml, 100 mM) with ammonia solution (0.5 M) added dropwise in the presence of polyvinylpyrrolidone (PVP) solution (0.1 mM) as a specific face-selective surfactant. The mixture became transparent. Aqueous solution of NaOH (0.3 ml, 2 M) was added to the colorless solution under vigorous stirring. The obtained Ag_2O was several times washed with distilled water and ethanol. At the second step, hydrogen peroxide (10 ml, 10%) was added as a reducing agent to Ag_2O under stirring followed by the injection of etching ammonia solution (10 ml, 0.5 M). The synthesized silver particles were collected by centrifugation.

[‡] Micrometer-sized single crystalline silver particles (coincided with the geometrical size of nanostructured silver octahedra) have never been used for SERS devices since such large particles are SERS ineffective and possess a small surface area.[3,10]

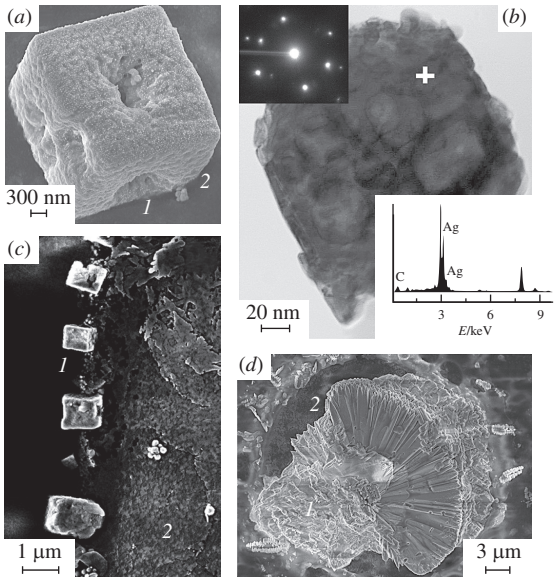

Figure 2 Complex morphology of nanostructured particles formed after the ultrasonic spray pyrolysis of aqueous diamminesilver(I) hydroxide: (*a*) SEM image of typical pseudomorphic cubes superficially decorated with Ag NPs, (*b*) TEM image, ED and local chemical analysis of the cubes, (*c*) SEM overall view of Ag NPs growth in the condensation zone showing (*1*) pseudomorphic cubes and (*2*) chaotically nucleated silver particles, and (*d*) SEM view of (*1*) porous silver bundle overgrown with (2) textured silver crystallites.

growth of solid phases providing usually a broad particle size distribution, however octahedral particles dominate certainly under the selected experimental conditions. The octahedral particles are the centres of silver regrowth and secondary nucleation upon the redox process as seen from additional silver seeds deposited onto facets of some octahedra. Each of the particles consists of silver clusters (20–40 nm) forming pseudomorph octahedral shapes with a large number of pores increasing partly the overall surface area and, what is even more important, most probably providing capillary channels for analytes to reach the 'hot spots' in the pseudomorphs. The pseudomorphs consist evidently of pure metallic silver without residual silver oxide and XRD texture (see Figure 1) evidencing for their disordered internal polycrystalline structure; the same is also confirmed indirectly by the presence of multiple nanosized pores and quite rough surface of the octahedra.¶

Oppositely, a thermal treatment of ultrasonic mist within a hot zone resulted in the irreversible decomposition of the major part of initial silver complex and also quick solvent evaporation followed by the formation of crystalline Ag_2O intermediate. The further pseudomorphic products of this transformation include silver nanostructured particles (see Figure 2), water, ammonia, and oxygen. Some molecular oxygen contacting the products was from surrounding air. Polyhedral aggregates could result from initial Ag_2O formation within the mist droplets prior its decomposition into silver and oxygen. Silver(I) oxide is capable of producing cubic, edge- and corner-truncated cubic, rhombicuboctahedral, edge- and corner-truncated octahedral, octahedral, and hexapod structures.[13] All of them could then transform into pure silver forming pores due to the oxygen release. As soon as liquid water and remaining traces of silver(I) complex reside together in the condensation zone at decreased temperature (60–80 °C), it facilitates the achievement of both superficial decoration with small Ag NPs and self-assembly of very complex, hierarchic silver micro- and nanostructures (see Figure 2) resembling the growth of skeleton forms of crystals under highly nonequilibrium conditions with a lack of nutrient phase. Thus, the flat facet growth was replaced with development of quickly growing rough grains and dendrites. The growth of 'porous bundles' and nanoflowers seems to be different steps of the same process of Ag_2O thermochemical transformation followed by kinetically controlled development of the fastest growing grains co-oriented at once due to the initial texture of bundles.

The silver cubes (see Figure 2) do not look as single crystalline species. Their size enlargement occurs due to the post-reduction of silver in the presence of remaining Ag^+ byproducts and overgrowth of the initial particles. The cubes could be thus considered as pseudocrystals formed in a topotactic manner preserving the shape of precursor crystals of Ag_2O. Their transformation demands oxygen loss, and this develops nanoporosity. Thermochemical etching and overgrowth are evident from the morphology of cubes. This assumption explains quite well the diversity in sizes and morphology of the cubes.

The unique nanostructures obtained by both the methods are favourable for their implementation into SERS devices since

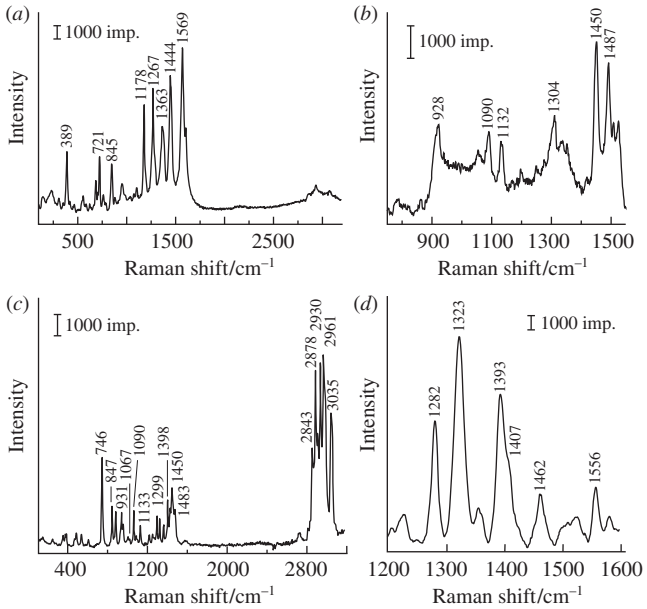

Figure 3 SERS spectra of (*a*) an absorbed layer of evaporated CHT and (*b*) aqueous meldonium, (*c*) reference spectrum of crystalline meldonium, and (*d*) SERS spectrum of highly diluted (10^{-10} M) Rhodamine 123 dye. Spectra (*a*),(*b*) were recorded using the prepared silver pseudomorphs (*via* reduction of Ag_2O octahedra) at 10% of nominal laser power and 1 μM concentrations for the acquisition time of 10–60 s, and spectrum (*d*) was recorded using nanostructured particles obtained after ultrasonic spray pyrolysis.

§ Diamminesilver(I) hydroxide was decomposed by aerosol spray pyrolysis. To prepare aqueous diamminesilver(I) hydroxide solutions for the aerosol protocol, aqueous (0.1 M) NaOH (Aldrich) was added dropwise to fresh aqueous silver nitrate solution (0.01 M) until the complete precipitation of black-brown Ag_2O. This as-prepared oxide was thoroughly washed with deionized water (high purity water, Milli-Q, Millipore) and dissolved in aqueous ammonia solution (10%, twofold molar excess) to give solution (0.03–0.3 M) of a silver(I) complex nebulized into a hot zone (550–950 °C) of a tubular furnace.

¶ The obtained materials were characterized by a transmission electron microscopy (TEM) and electron diffraction (ED) using LEO912 AB OMEGA (Carl Zeiss) and Jeol JEM 2100F (Jeol) instruments. The pristine sample microstructure was studied using a Carl Zeiss NVision 40 field emission scanning electron microscope at the accelerating voltage of 0.5–5 kV. The obtained substrates were examined using a Rigaku D/MAX 2500 (Japan) instrument equipped with a rotating copper anode (CuKα irradiation, 2θ range of 5–80°, and step of 0.02°). Raman and SERS experiments were performed using an InVia Raman microscope (Renishaw, UK) equipped with an argon laser (20 mW, 514 nm) and power neutral density filter (10%). All the spectra were collected using 20× objective lens for the acquisition time of 10–120 s. A silicon wafer was employed for the calibration.

they reveal a pronounced effect of Raman scattering enhancement. Figure 3 shows typical SERS spectra of the model dye (Rhodamine 123), oil pollutant and pharmaceutical compound.[††] In the case of Rhodamine 123, all major peaks were recorded at the lowest detection threshold of about 0.1–0.05 nM. This concentration is not detectable by a conventional Raman spectroscopy, but millimolar concentrations start to manifest the intense fluorescence of rhodamine. This SERS effectiveness of the produced materials confirms that they are composed of nanostructured metallic silver as was also observed by TEM, EDX, XRD and electron diffraction patterns (see Figure 2).

The octahedral particles produced *via* the PVP protocol plays the role of a highly hierarchic structure being ready for SERS applications (see Figure 3) for model dye analytes, molecular thiol products, crude oil desulfurization markers, and also for well-known pharmaceutical compounds like meldonium [mildronate, 3-(2,2,2-trimethyldiazan-2-ium-1-yl)propanoate]. In particular, the SERS spectrum of cyclohexanethiol (CHT) represents its adsorbed layers anchored onto silver surface *via* the thiol groups. The S–H stretching band usually appearing at 2570 cm^{-1} and also the CSH bending mode at 800–900 cm^{-1} are missing in the SERS spectra indicating that the molecules are dissociatively adsorbed on the silver surface forming a link to the silver. Oppositely, the band at 721 cm^{-1} corresponds to the C–S stretching due to the interaction with silver. Other vibration modes are typical for the various conformers of cyclohexane ring: ring deformation and stretching at 389 and 845 cm^{-1}, and CH_2 twisting, wagging, scissoring and stretching at 1178, 1267, 1363, 1444, 2900 cm^{-1}. Meldonium species can be detected in water at the micromolar levels (see Figure 3). Evidently, the most of bright vibrational modes are present in both the original and enhanced Raman spectra with varied intensities depending, as in the case of CHT, on the conformations of absorbed molecules.

In conclusion, various production protocols of silver pseudomorphs from aqueous diamminesilver(I) hydroxide opened up a new simple access to the nanostructured particles possessing desired morphologies for practical applications. The growth features seem to be related to the decomposition of diamminesilver(I) hydroxide *via* Ag_2O as the intermediate and its further reduction into pure silver. Aqueous diamminesilver(I) hydroxide as compared to other salts and complexes provides a large benefit owing to simplicity, promptness and low temperature conditions of the preparation process. The latter allows one, in particular, to obtain nanoparticles with new types of morphologies suitable for SERS measurements for the analysis of oil pollutants and pharmaceutical substances.

This work was supported in its instrumental part by the M. V. Lomonosov Moscow State University Program of Development. EAG acknowledges the support by the Russian Science Foundation (grant no. 14-13-00871). AAS was supported by the Grant of the President of the Russian Federation for the governmental support of young scientists (grant no. MK-1146.2017.3).

References

1 R. A. Alvarez-Puebla and L. M. Liz-Marzán, *Small*, 2010, **6**, 604.
2 B. Pietrobon and V. Kitaev, *Chem. Mater.*, 2008, **20**, 5186.
3 S. Hong and X. Li, *J. Nanomater*., 2013, Article ID 790323, http://dx.doi.org/10.1155/2013/790323.
4 N. Leopold and B. Lendl, *J. Phys. Chem. B*, 2003, **107**, 5723.
5 J. Kneipp, H. Kneipp, B. Wittig and K. Kneipp, *Nano Lett.*, 2007, **7**, 2819.
6 Yu. M. Maksimov, B. I. Podlovchenko, E. M. Gallyamov, S. A. Dagesyan, V. V. Sen and S. A. Evlashin, *Mendeleev Commun.*, 2017, **27**, 382.
7 L. B. Gulina, V. P. Tolstoy and E. V. Tolstobrov, *Mendeleev Commun.*, 2017, **27**, 634.
8 B. R. Wood, P. Caspers, G. J. Puppels, S. Pandiancherri and D. McNaughton, *Anal. Bioanal. Chem.*, 2007, **387**, 1691.
9 O. E. Eremina, A. A. Semenova, E. A. Sergeeva, N. A. Brazhe, G. V. Maksimov, T. N. Shekhovtsova, E. A. Goodilin and I. A. Veselova, *Russ. Chem. Rev.*, 2018, **87**, 741.
10 R. X. He, R. Liang, P. Peng and Y. N. Zhou, *J. Nanopart. Res.*, 2017, **19**, 267.
11 A. M. Ermakova, J. E. Morozova, Ya. V. Shalaeva, V. V. Syakaev, I. R. Nizameev, M. K. Kadirov, I. S. Antipin and A. I. Konovalov, *Mendeleev Commun.*, 2017, **27**, 335.
12 A. Guerrero-Martínez, S. Barbosa, I. Pastoriza-Santos and L. M. Liz-Marzán, *Curr. Opin. Colloid Interface Sci.*, 2011, **16**, 118.
13 J. Fang, S. Liu and Z. Li, *Biomaterials*, 2011, **32**, 4877.
14 E. Thimsen, *Chem. Mater.*, 2011, **23**, 4612.
15 N. A. Brazhe, A. B. Evlyukhin, E. A. Goodilin, A. A. Semenova, S. M. Novikov, S. I. Bozhevolnyi, B. N. Chichkov, A. S. Sarycheva, A. A. Baizhumanov, E. I. Nikelshparg, L. I. Deev, E. G. Maksimov, G. V. Maksimov and O. Sosnovtseva, *Sci. Rep.*, 2015, **5**, 13793.
16 A. A. Semenova, A. P. Semenov, E. A. Gudilina, G. T. Sinyukova, N. A. Brazhe, G. V. Maksimov and E. A. Goodilin, *Mendeleev Commun.*, 2016, **26**, 177.
17 A. A. Semenova, E. A. Goodilin, N. A. Brazhe, V. K. Ivanov, A. E. Baranchikov, V. A. Lebedev, A. E. Goldt, O. V. Sosnovtseva, S. V. Savilov, A. V. Egorov, A. R. Brazhe, E. Y. Parshina, O. G. Luneva, G. V. Maksimov and Y. D. Tretyakov, *J. Mater. Chem.*, 2012, **22**, 24530.
18 P. J. Yunker, T. Still, M. A. Lohr and A. G. Yodh, *Nature*, 2011, **476**, 308.
19 G. Haran, *Acc. Chem. Res.*, 2010, **43**, 1135.
20 A. A. Semenova, V. K. Ivanov, S. V. Savilov and E. A. Goodilin, *CrystEngComm*, 2013, **15**, 7863.

Received: 7th December 2018; Com. 18/5764

[††] The enhancement factors (EF) were calculated as the ratio of corresponding peak intensities for SERS and RS measurements divided by the ratio of corresponding concentrations. EF for Rhodamine 123 dye reached $0.5–1.0 \times 10^8$, while EF for meldonium and CHT were estimated as $0.7–1.2 \times 10^6$.